Light-induced magnetization in a spin $S = 1$ easy-plane antiferromagnetic chain

J. Herbrych[1] and X. Zotos[1,2,3]

[1]*Cretan Center for Quantum Complexity and Nanotechnology and Institute of Theoretical and Computational Physics, Department of Physics, University of Crete, Heraklion 71003, Greece*

[2]*Foundation for Research and Technology–Hellas, 71110 Heraklion, Greece*

[3]*Max-Planck-Institut für Physik komplexer Systeme, Nöthnitzer Strasse 38, 01187 Dresden, Germany*

(Received 12 May 2015; revised manuscript received 3 July 2015; published 11 April 2016)

The time evolution of magnetization induced by circularly polarized light in an $S = 1$ Heisenberg chain with large easy-plane anisotropy is studied numerically and analytically. Results at constant light frequency $\Omega = \Omega_0$ are interpreted in terms of absorption lines of the electronic spin resonance spectrum. The application of time-dependent frequency $\Omega = \Omega(t)$ light, so called chirping, is shown to be an efficient procedure in order to obtain within a short time a large, controlled value of the magnetization M^z. Furthermore, comparison with a two-level model provides a qualitative understanding of the induced magnetization process.

DOI: 10.1103/PhysRevB.93.134412

Far-from-equilibrium condensed-matter physics is challenging and still largely uncharted territory. With regard to the out-of-equilibrium dynamics of quantum magnets, the control of magnetic properties by means other than a conventional magnetic field is of strong current interest [1–5]. For instance, engineering the quantum state, i.e., the wave function, is essential for quantum simulators, precision sensors, or spintronic devices [6–10]. Recent experimental advances have allowed us to manipulate the elementary low-energy excitations with terahertz laser pulses [11–15], a prominent example being the ultrafast coherent control of antiferromagnetic magnons. A time-dependent (rotating) magnetic field of highly intense terahertz laser pules, with photon energy below the electron energy scale, controlled the coherent spin waves without interfering with the motion of charge carriers.

In quantum magnets with reduced dimensionality, the thermodynamic and transport properties exhibit a rich magnetic-field dependence [16–23] related to the total magnetization of the system. Prominent examples of such behavior are the field-induced quantum phase transitions of the organic compound $NiCl_2$-4SC$(NH_2)_2$ (dichlorotetrakisthiourea-nickel, abbreviated as DTN). At zero temperature, the first transition occurs at a critical field h_1 where the energy gap closes and a finite magnetization develops in the ground state (GS); the second one occurs at h_2 where the magnetization fully saturates, leading to a ferromagnetic GS. By now, the low-energy physics of the DTN compound has been well studied experimentally [16,22–26] and understood theoretically. The basic model that describes the magnetic excitation spectrum of DTN was found to be the one-dimensional $S = 1$ antiferromagnetic Heisenberg model (AHM) with exchange coupling constant J and large easy-plane anisotropy D. As shown in Refs. [27–30], such a Hamiltonian reproduces in great detail the low-lying electronic spin resonance (ESR) spectrum. The anisotropy $D/J \sim 4$ of DTN, being the largest energy scale in the system, is responsible for a large energy gap $O(D)$ that can be closed by a magnetic field h.

In this work, we study the rotating magnetic-field-induced nonequilibrium magnetization M^z in a large, easy-plane anisotropy AHM. For a field rotating at constant frequency (circularly polarized light), we are connecting the numerical results with the linear-response (LR) theory predictions for the transition frequency of the corresponding ESR experiment. In the case of a chirped (time-dependent) frequency of the light [31], our results indicate that the short-time behavior of the magnetization is mainly driven by the anisotropy part of the system. This time scale, together with the dependence of the magnetization on the chirp parameters, can be accurately described by a two-level model. The dynamics beyond the characteristic time of the latter is dominated by the Heisenberg part of the model. Although we focus on DTN as a typical one-dimensional $S = 1$ easy-plane AHM, our analysis is also valid for other Hamiltonians, e.g., a two-level model will yield the correct physics for $S = 1$ models in all dimensions provided that $D \gg J$.

As a prototype model, we choose the $S = 1$ AHM with single-site, easy-plane anisotropy D on a chain with L sites,

$$H_0 = \sum_{i=1}^{L} \left[J\mathbf{S}_i \cdot \mathbf{S}_{i+1} + D\left(S_i^z\right)^2 + hS_i^z \right], \tag{1}$$

where $\mathbf{S}_i = (S_i^x, S_i^y, S_i^z)$ are spin $S = 1$ operators at site i, $\mathbf{S}_{L+1} = \mathbf{S}_1$ (periodic boundary conditions), h is a magnetic field, and J ($\sim$2 K) is the antiferromagnetic exchange constant (later we will use $\hbar = k_B = \mu_B = 1$ and set $J = 1$ as the unit of energy). Hereafter, we will use $D = 4$ ($\sim$8 K), and for such an anisotropy the critical fields are $h_1 \simeq 2.28$ and $h_2 = 8$ [28]. We will assume that only the magnetic component of light, propagating in the z direction, couples to the system. The time-dependent Hamiltonian of the corresponding setup can be written as

$$H(t) = H_0 - A \sum_{i=1}^{L} (e^{-i\Omega t} S_i^+ + e^{i\Omega t} S_i^-), \tag{2}$$

where $A > 0$ and $\Omega > 0$ are the amplitude and frequency of light, respectively, and $S_i^{\pm}$ are spin-raising and -lowering operators. Thus, each spin "feels" a magnetic field rotating in the xy plane, $2A \sum_i [S_i^x \cos(\Omega t) + S_i^y \sin(\Omega t)]$. The magnetization induced is positive. To obtain a negative magnetization, one should substitute $\Omega \to -\Omega$ in (2). Note that in a real experiment, a propagating light pulse has some time and frequency dependence, an issue that we will discuss later on. To probe the sample magnetization perpendicular to

the polarization plane, one can use a second optical pulse and measure the change in its polarization state induced by the magnetization either in transmission (Faraday effect) or reflection (Kerr effect) geometry [2,13,32].

The time evolution of the magnetization is given by

$$M^z(t) = \frac{\langle\Psi(t)|S^z_{\rm tot}|\Psi(t)\rangle}{\langle\Psi(t)|\Psi(t)\rangle}, \tag{3}$$

where $S^z_{\rm tot} = (1/L)\sum_i S^z_i$, and $|\Psi(t)\rangle$ is a solution of the time-dependent Schrödinger equation $i\partial_t|\Psi(t)\rangle = H(t)|\Psi(t)\rangle$. In our calculation, we choose δt in such a way that typically $\langle\Psi(t)|\Psi(t)\rangle \simeq 1$ at any time t ($\delta t \simeq 10^{-3}$). A general procedure goes as follows: (i) first, with help from exact diagonalization we calculate the GS of (1), $|\Psi(-\delta t)\rangle = |{\rm GS}\rangle$; (ii) next, at time $t = 0$ we instantaneously turn on the light; and (iii) finally we perform the time evolution of it on the basis of the time-discretized version of the Schrödinger equation with (2) (using a fourth-order Runge-Kutta routine).

Let us first focus on the system (2) at constant frequency $\Omega = \Omega_0$. It is clear that the maximum value of the magnetization is induced by light at the resonance frequency of the system, $\Omega_0 = \Omega_R$, which can be interpreted in the spirit of an ESR spectrum. For small enough A ($\ll J$) the system is in the linear-response regime and the low absorption lines of the ESR spectrum of (1) [28,33] correspond to the resonance frequencies Ω_R of (2) at given h. Furthermore, (2) at $\Omega = \Omega_0$ can be mapped by a unitary transformation (or Floquet theory) to an effective static model [34–36], where the latter has a form similar to the one when dealing with an ESR experiment. Note that the same procedure was used in Ref. [34] in order to study a system with small magnetic anisotropy $D = 0.25$ (the Haldane-like limit).

Figure 1(a) depicts a typical example of the time dependence of M^z as a function of time for a system with $h = 0$ and constant Ω. Several conclusions can be drawn directly from the obtained results: (i) It is evident that the M^z induced by $\Omega_0 = \Omega_R$ is dominating above other frequencies. (ii) The beating frequency presented in the inset of Fig. 1(a) is attributed to finite-size effects. (iii) The value of $\Omega_R = 6$ for $h = 0$ is consistent with the lowest transition lines of the ESR spectrum. In fact, in the gapless regime $h < h_1$, the ESR lines can be calculated by a $1/D$ expansion [27,28], i.e.,

$$\omega_A = D + 2J + h\,, \quad \omega_B = D + 2J - h\,.$$

Such lines correspond to transitions from the GS to states with $\Delta S^z = \pm 1$.

In Fig. 1(b) we present a heat map of the average (over the time span $\delta t < t < 100$) net magnetization, $\overline{M^z} - M^z(t = 0)$, as a function of magnetic field h and frequency Ω_0. Our results perfectly reproduce both ESR predictions, e.g., see Fig. 6 of Ref. [28]. In the considered field h region we also see a continuation of the $\omega_G = D + h$ line—transitions from a magnon to a single-ion bound state. Other resonance lines can also be captured, e.g., transitions from the fully ordered ferromagnetic state in the $h > h_2$ region can be resolved by looking for Ω_R of negative magnetization. In Fig. 2(a), we present $M^z(t = 5)$ as a function of frequency Ω_0. The maximum value of magnetization for given h and $\Omega > 0$, or $\Omega < 0$, is consistent with the ESR predictions.

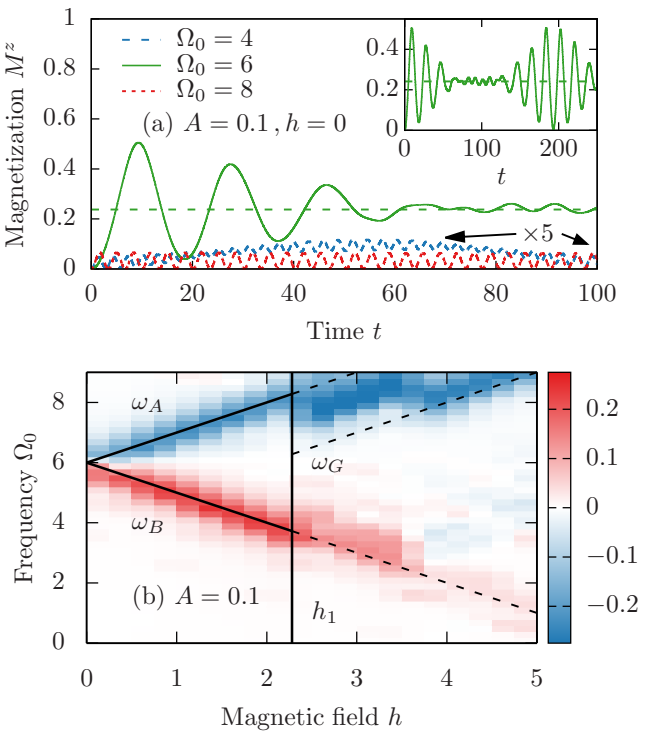

FIG. 1. (a) Magnetization as a function of time $M^z(t)$ calculated for $L = 11$, $A = 0.1$, $h = 0$, and $\Omega_0 = 4,6,8$. The dashed horizontal line represents the average value for $\Omega_0 = 6$. Note that the results for $\Omega_0 = 4$ and 8 are multiplied by factor of 5 for clarity. Inset: $M^z(t)$ induced by $\Omega_0 = \Omega_R = 6$ (as in the main panel) for t up to $t = 250$. (b) Heat map of average net magnetization, $\overline{M^z} - M^z(t = 0)$, as a function of magnetic field h and frequency Ω_0, calculated for $L = 10\,, A = 0.1$. ω_B line (red color in the heat map) is obtained with $\Omega > 0$ in (2), $\omega_{A,G}$ (blue color) with $\Omega < 0$. Solid and dashed lines represent the $\omega_{A,B,G}$ ESR resonance lines and their continuation into the gapless regime. The vertical solid line represents the critical field h_1.

Although we chose the GS as the starting point of the time evolution, this is not a zero-temperature ($T = 0$) result. Within LR theory, one would expect for $T = 0$ rather sharp transition lines [29]. It is clear from Fig. 1(b) that our resonance lines are not δ peaks, with nonzero intensity for all considered transitions $\omega_{A,B,G}$. Also, in Fig. 2(b) we present the dependence of $h = 0$ average magnetization $\overline{M^z}$ on frequency Ω_0 for various amplitudes $A = 0.01,0.05,0.1,0.5$ in (2). Within LR such a broadening of the line could be interpreted as an increase of the effective temperature.

Next, in order to induce macroscopic magnetization in a controlled way, we study the application of a chirped pulse, $\Omega = \Omega(t)$. Although the time dependence of Ω can be complicated and its functional form dependent on the experimental setup, the main features should be captured by the simple form

$$\Omega(t) = \Omega_I - \nu t, \tag{4}$$

where Ω_I is the initial ($t = 0$) frequency and ν is the chirp, i.e., the "speed" of frequency change. Within such a notation, $\Omega_I = \Omega_R$ and $\nu = 0$ corresponds to a time-independent Ω at the resonance frequency. In the following, we will consider

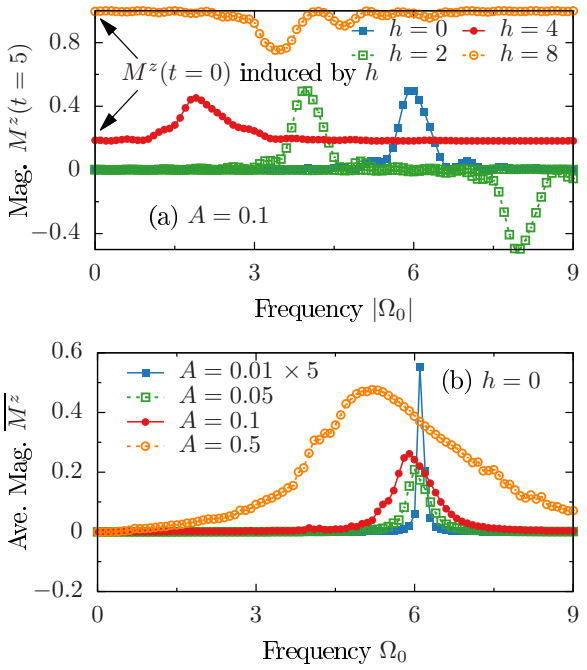

FIG. 2. (a) Frequency Ω_0 dependence of the magnetization M^z at time $t = 5$ and $L = 11$. Results for $h = 0,2,4$ are calculated with $\Omega_0 > 0$ (positive magnetization) and for $h = 2,8$ with $\Omega_0 < 0$ (negative magnetization). Note that for $h > h_1$ (presented for $h = 4,8$) the ground state has net magnetization already at $t = 0$. (b) Frequency dependence of average magnetization $\overline{M^z}$ for $h = 0$, $L = 11$ and various amplitudes $A = 0.01,0.05,0.1,0.5$. Results for $A = 0.01$ are multiplied by factor of 5 for clarity.

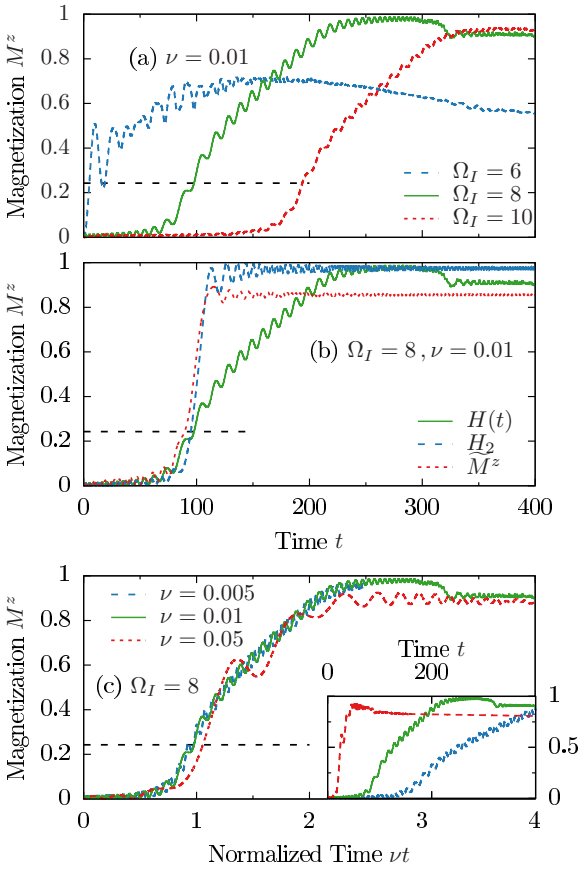

FIG. 3. Time dependence of the magnetization calculated for $L = 11$, $h = 0$, and $A = 0.1$. (a) Magnetization as a function of time calculated for various initial frequencies $\Omega_I = 6,8,10$ and $\nu = 0.01$. The horizontal line represents the average value of magnetization for $\nu = 0$ and $\Omega_I = \Omega_R = 6$ (resonance frequency). (b) Comparison of the magnetization as calculated with Eq. (3) for (i) the full Hamiltonian (2) with $\Omega_I = 8\,, \nu = 0.01$, and (ii) the two-level model (5) and the perturbative solution $\widetilde{M}^z$—Eq. (6) with $\Delta = 2$, $\nu = 0.01$. (c) Magnetization as a function of normalized time νt for $\nu = 0.005,0.01,0.05$, initial frequency $\Omega_I = 8$, and $A = 0.1$. Inset: the same results as a function of time t.

only the $h = 0$ case, i.e., $\Omega_R = 6$, as we would like to study the magnetization induced only by light.

The qualitative dependence of the magnetization on the amplitude A and chirping ν can be understood within a two-level model,

$$H_2 = 0|0\rangle\langle 0| + D|1\rangle\langle 1| + \sqrt{2}A(e^{-i\Omega t}|1\rangle\langle 0| + \text{H.c.}), \quad (5)$$

where $|0\rangle$ ($|1\rangle$) corresponds to the $S_i^z = 0(1)$ states of the term $D(S_i^z)^2$, relevant to the $J/D \to 0$ limit of (1). Note that the resonance frequency of (5) is simply $\Omega_R = D$. Within this model, a perturbative expression, $\alpha = A/\sqrt{\nu} \to 0$, of the time dependence of the magnetization can be given as

$$\widetilde{M}^z(t) = \frac{|W(t)|^2}{1+|W(t)|^2},$$
$$W(t) = \sqrt{2}A\int_0^t dt'\, e^{-i(\Delta-\nu t')t'}$$
$$= \sqrt{2}\alpha\, e^{-i\Delta^2/4\nu}\int_0^{t\sqrt{\nu}} m d\tau\, e^{+i(\tau-\frac{\Delta}{2\sqrt{\nu}})^2}, \quad (6)$$

where $\Delta = \Omega_I - \Omega_R$. It is obvious from the above equation that $\widetilde{M}^z(t)$ depends only on α and the detuning Δ.

In Fig. 3(a) we present the magnetization dependence on the initial frequency Ω_I at fixed ν. In panel (b) we present numerical results obtained from the full Hamiltonian (2), the two-level model (5) with corresponding detuning, together with the perturbative solution Eq. (6), which captures the main features of the magnetization profile. Note that the results are indistinguishable until the saddle point of Eq. (6), i.e., at $t_s = \Delta/2\nu$. From the results presented in Fig. 3(b) it is obvious that the main effect of the exchange coupling J is in the dynamics of the magnetization at times t beyond t_s. It is also interesting to note that the magnetization induced by a constant frequency light $\Omega = \Omega_R$, as indicated by a dashed line in Fig. 3, is reached at the saddle-point time t_s. We observe such behavior for all $\Omega_I > \Omega_R$.

In Fig. 3(c) we show the time dependence of the induced magnetization for different chirping speeds ν. We observe that (i) in the scaled time νt the curves are practically identical with the crossing of the mean value at $\nu = 0$ and $\Omega_I = \Omega_R$ at $\nu t \sim \nu t_s = 1$, reaching maximum at $\nu t \sim 2$; (ii) the magnetization at long times is weakly dependent on time, a remarkable result considering that we are dealing with a full many-body problem, where a decay could be expected; and (iii) it is clear that, as the total magnetization $S^z = \sum_i S_i^z$ commutes with the Hamiltonian, after switching off the light at a certain time, M^z remains constant at its instantaneous

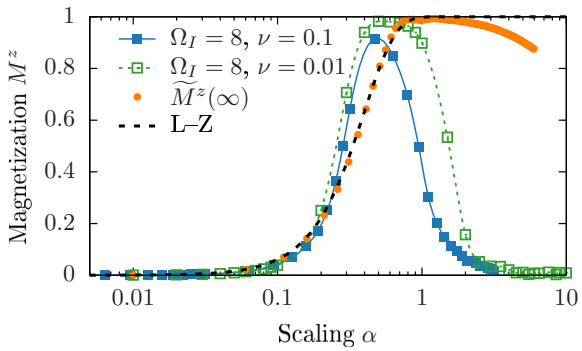

FIG. 4. Scaling parameter $\alpha = A/\sqrt{\nu}$ dependence of the magnetization as calculated for $L = 11$, $\nu = 0.1$ (full squares), and $\nu = 0.01$ (open squares). The snapshot of magnetization of the full model (squares) is taken at $\nu t = 2$, i.e., $t = 20$ for $\nu = 0.1$ and $t = 200$ for $\nu = 0.01$. Circles represent the magnetization $\widetilde{M}^z(\infty)$ dependence on α in the two-level model (5) and the black dashed line depicts the Landau-Zener expression.

value. This allows for a tight control of the value of the induced magnetization in the system. Further simulations for different $\Omega_I > \Omega_R$ confirm this picture; crossing the resonance frequency by chirping the light frequency induces a stable macroscopic magnetization in the system. Additionally, it is clear from the solution of the two-level model that inverting $\Delta' = -\Delta$ and $\nu' = -\nu$ produces an identical evolution of magnetization.

Considering the amplitude and chirping speed dependence of the long-time asymptotic magnetization achieved, first of all we observe that the two-level model can be mapped in a rotating frame to a Landau-Zener-type tunneling problem,

$$\widetilde{H}_2 = \widetilde{\Delta}|\widetilde{1}\rangle\langle\widetilde{1}| - \widetilde{\Delta}|\widetilde{0}\rangle\langle\widetilde{0}| + \sqrt{2}A(|\widetilde{1}\rangle\langle\widetilde{0}| + \text{H.c.}), \quad (7)$$

where $\widetilde{\Delta} = \Delta/2 - \nu t$. In the Landau-Zener problem, $\Delta = 0$ and the time evolution is from $t = -\infty$ to $+\infty$, while in the situation we are considering the time evolution starts at $t = 0$ and from a finite frequency shift Δ. For $\Delta/\nu \gg 1$, the asymptotic $\widetilde{M}^z(\infty)$ coincides with the probability of occupation of level $|1\rangle$ given by the Landau-Zener expression $1 - \exp(-\pi\alpha^2)$.

In Fig. 4 we present a comparison of the long-time magnetization ($\nu t = 2$) in the full model (2), the perturbative prediction Eq. (6), and the Landau-Zener expression. Note that although $\widetilde{M}^z$ is a perturbative solution ($\alpha \to 0$) and the detailed dynamics beyond t_s is not captured correctly [see Fig. 3(b)], the overall agreement of the asymptotic magnetization is qualitatively described until $\alpha \sim 1$ [36].

Finally, turning to the experimental realization, for the DTN compound ($J = 2.2$ K, $D = 8.9$ K) the resonance frequency is $\Omega_R \approx 300$ GHz. Light of magnetic field intensity $\approx$0.3 T corresponding to an electric field of $\approx$1 MV/cm and a chirping speed $\nu \approx 0.1$ will induce a controlled macroscopic magnetization within $\approx$1 ps [37]. In a realistic experimental situation, several issues arise: (i) in terahertz spectroscopy, the light is in the form of a pulse of duration $\approx$1 ps; (ii) the effect of the electric field should be estimated; (iii) experiments are at a finite temperature; and (iv) there is spin-lattice relaxation that could be detrimental to the process of inducing macroscopic magnetization. However, it is known that in several quantum magnets [38] the relaxation time is surprisingly long. Preliminary finite-temperature simulations and considerations are encouraging in rendering the proposed experiment feasible. We should also note that the large variety of quantum magnets allow for a tailoring of the experiments in terms of light frequency, relaxation time, etc.

In summary, we have studied an efficient protocol that induces magnetization without an external magnetic field applied to the system. The results for a circularly polarized light pulse at constant frequency are explained with the help of resonance lines of ESR transitions at finite temperature. We have also presented comprehensive results on the dependence of the magnetization on a chirped pulse. The latter, experimentally relevant, protocol can be qualitatively and even for some time scales quantitatively described with the help of a two-level model. Also, it was shown [29] that (1) can be mapped to an effective $S = 1/2$ AHM with exchange anisotropy < 1. Our two-level predictions for this model will be even more accurate since the mapping favors the large-D limit.

This work was supported by the European Union program FP7-REGPOT-2012-2013-1 under Grant Agreement No. 316165 and by the European Union (European Social Fund, ESF), Greek national funds through the Operational Program "Education and Lifelong Learning" of the NSRF under "Funding of proposals that have received a positive evaluation in the 3rd and 4th call of ERC Grant Schemes." We acknowledge helpful and inspiring discussions with R. Steinigeweg, W. Brenig, P. Prelovšek, Z. Lenarčič, S. Miyashita, P. van Loosdrecht, M. Montagnese, B. Büchner, C. Hess, V. Kataev, S. Takayoshi, and T. Oka.

[1] A. Asamitsu, Y. Tomioka, H. Kuwahara, and Y. Tokura, Nature (London) **388**, 50 (1997).
[2] Y. Kato, R. C. Myers, A. C. Gossard, and D. D. Awschalom, Nature (London) **427**, 50 (2004).
[3] T. Lottermoser, Nature (London) **430**, 541 (2004).
[4] A. V. Kimel, A. Kirilyuk, P. A. Usachev, R. V. Pisarev, A. M. Balbashov, and T. Rasing, Nature (London) **435**, 655 (2005).
[5] S. Hild, T. Fukuhara, P. Schauß, J. Zeiher, M. Knap, E. Demler, I. Bloch, and C. Gross, Phys. Rev. Lett. **113**, 147205 (2014).
[6] B. E. Cole, J. B. Williams, B. T. King, M. S. Sherwin, and C. R. Stanley, Nature (London) **410**, 60 (2001).
[7] C. Nayak, S. H. Simon, A. Stern, M. Freedman, and S. Das Sarma, Rev. Mod. Phys. **80**, 1083 (2008).
[8] J. Simon, W. S. Bakr, R. Ma, M. E. Tai, P. M. Preiss, and M. Greiner, Nature (London) **472**, 307 (2011).
[9] J. W. Britton, B. C. Sawyer, A. C. Keith, C.-C. J. Wang, J. K. Freericks, H. Uys, M. J. Biercuk, and J. J. Bollinger, Nature (London) **484**, 489 (2012).
[10] A. Stern and N. H. Lindner, Science **339**, 1179 (2013).

[11] R. Huber, F. Tauser, A. Brodschelm, M. Bichler, G. Abstreiter, and A. Leitenstorfer, Nature (London) **414**, 286 (2001).
[12] A. Kirilyuk, A. V. Kimel, and T. Rasing, Rev. Mod. Phys. **82**, 2731 (2010).
[13] T. Kampfrath, A. Sell, G. Klatt, A. Pashkin, S. Mährlein, T. Dekorsy, M. Wolf, M. Fiebig, A. Leitenstorfer, and R. Huber, Nat. Photon. **5**, 31 (2011).
[14] E. Beaurepaire, G. M. Turner, S. M. Harrel, M. C. Beard, J.-Y. Bigot, and C. A. Schmuttenmaer, Appl. Phys. Lett. **84**, 3465 (2004).
[15] S. Takahashi, J. van Tol, C. C. Beedle, D. N. Hendrickson, L.-C. Brunel, and M. S. Sherwin, Phys. Rev. Lett. **102**, 087603 (2009).
[16] V. S. Zapf, D. Zocco, B. R. Hansen, M. Jaime, N. Harrison, C. D. Batista, M. Kenzelmann, C. Niedermayer, A. Lacerda, and A. Paduan-Filho, Phys. Rev. Lett. **96**, 077204 (2006).
[17] A. V. Sologubenko, T. Lorenz, H.-R. Ott, and A. Freimuth, J. Low Temp. Phys. **147**, 387 (2007).
[18] A. V. Sologubenko, K. Berggold, T. Lorenz, A. Rosch, E. Shimshoni, M. D. Phillips, and M. M. Turnbull, Phys. Rev. Lett. **98**, 107201 (2007).
[19] M. Klanjšek, H. Mayaffre, C. Berthier, M. Horvatić, B. Chiari, O. Piovesana, P. Bouillot, C. Kollath, E. Orignac, R. Citro, and T. Giamarchi, Phys. Rev. Lett. **101**, 137207 (2008).
[20] A. V. Sologubenko, T. Lorenz, J. A. Mydosh, A. Rosch, K. C. Shortsleeves, and M. M. Turnbull, Phys. Rev. Lett. **100**, 137202 (2008).
[21] A. V. Sologubenko, T. Lorenz, J. A. Mydosh, B. Thielemann, H. M. Rønnow, C. Rüegg, and K. W. Krämer, Phys. Rev. B **80**, 220411 (2009).
[22] X. F. Sun, W. Tao, X. M. Wang, and C. Fan, Phys. Rev. Lett. **102**, 167202 (2009).
[23] Y. Kohama, A. V. Sologubenko, N. R. Dilley, V. S. Zapf, M. Jaime, J. A. Mydosh, A. Paduan-Filho, K. A. Al-Hassanieh, P. Sengupta, S. Gangadharaiah, A. L. Chernyshev, and C. D. Batista, Phys. Rev. Lett. **106**, 037203 (2011).
[24] S. A. Zvyagin, J. Wosnitza, C. D. Batista, M. Tsukamoto, N. Kawashima, J. Krzystek, V. S. Zapf, M. Jaime, N. F. Oliveira Jr., and A. Paduan-Filho, Phys. Rev. Lett. **98**, 047205 (2007).
[25] S. A. Zvyagin, C. D. Batista, J. Krzystek, V. S. Zapf, M. Jaime, A. Paduan-Filho, and J. Wosnitza, Physica B **403**, 1497 (2008).
[26] S. Mukhopadhyay, M. Klanjšek, M. S. Grbić, R. Blinder, H. Mayaffre, C. Berthier, M. Horvatić, M. A. Continentino, A. Paduan-Filho, B. Chiari, and O. Piovesana, Phys. Rev. Lett. **109**, 177206 (2012).
[27] N. Papanicolaou, A. Orendáčová, and M. Orendáč, Phys. Rev. B **56**, 8786 (1997).
[28] C. Psaroudaki, S. A. Zvyagin, J. Krzystek, A. Paduan-Filho, X. Zotos, and N. Papanicolaou, Phys. Rev. B **85**, 014412 (2012).
[29] C. Psaroudaki, J. Herbrych, J. Karadamoglou, P. Prelovšek, X. Zotos, and N. Papanicolaou, Phys. Rev. B **89**, 224418 (2014).
[30] V. Zapf, M. Jaime, and C. D. Batista, Rev. Mod. Phys. **86**, 563 (2014).
[31] S. Zamith, J. Degert, S. Stock, B. de Beauvoir, V. Blanchet, M. A. Bouchene, and B. Girard, Phys. Rev. Lett. **87**, 033001 (2001).
[32] J. P. van der Ziel, P. S. Pershan, and L. D. Malmstrom, Phys. Rev. Lett. **15**, 190 (1965).
[33] M. Oshikawa and I. Affleck, Phys. Rev. Lett. **82**, 5136 (1999).
[34] S. Takayoshi, H. Aoki, and T. Oka, Phys. Rev. B **90**, 085150 (2014).
[35] S. Takayoshi, M. Sato, and T. Oka, Phys. Rev. B **90**, 214413 (2014).
[36] We should note that in Ref. [34] a similarly driven system with weak easy-axis anisotropy and no chirping was considered resulting in a rather small induced magnetization, while in Ref. [35] a description in terms of the Landau-Zener tunneling problem was presented in systems with $\Omega(t) = \nu t$, $\nu \sim 10^{-4}$, and a small symmetry-breaking anisotropy term giving $\Omega_R = O(0.1)$.
[37] P. van Loosdrecht and M. Montagnese (private communication).
[38] M. Montagnese, M. Otter, X. Zotos, D. A. Fishman, N. Hlubek, O. Mityashkin, C. Hess, R. Saint-Martin, S. Singh, A. Revcolevschi, and P. H. M. van Loosdrecht, Phys. Rev. Lett. **110**, 147206 (2013).